



LUND UNIVERSITY

The effect of curing conditions on chloride ingress in concrete

Johannesson, Björn

2000

[Link to publication](#)

Citation for published version (APA):

Johannesson, B. (2000). *The effect of curing conditions on chloride ingress in concrete*. (Report TVBM; Vol. 3094). Division of Building Materials, LTH, Lund University.

Total number of authors:

1

General rights

Unless other specific re-use rights are stated the following general rights apply:

Copyright and moral rights for the publications made accessible in the public portal are retained by the authors and/or other copyright owners and it is a condition of accessing publications that users recognise and abide by the legal requirements associated with these rights.

- Users may download and print one copy of any publication from the public portal for the purpose of private study or research.
- You may not further distribute the material or use it for any profit-making activity or commercial gain
- You may freely distribute the URL identifying the publication in the public portal

Read more about Creative commons licenses: <https://creativecommons.org/licenses/>

Take down policy

If you believe that this document breaches copyright please contact us providing details, and we will remove access to the work immediately and investigate your claim.

LUND UNIVERSITY

PO Box 117
221 00 Lund
+46 46-222 00 00

LUND INSTITUTE OF TECHNOLOGY
LUND UNIVERSITY

Division of Building Materials

The Effect of Curing Conditions on Chloride Ingress in Concrete

Björn Johannesson



TVBM-3094

Lund 2000

LUND INSTITUTE OF TECHNOLOGY
LUND UNIVERSITY

Division of Building Materials

The Effect of Curing Conditions on Chloride Ingress in Concrete

Björn Johannesson

ISRN LUTVDG/TVBM--00/3094--SE(1-40)
ISSN 0348-7911 TVBM

Lund Institute of Technology
Division of Building Materials
Box 118
SE-221 00 Lund, Sweden

Telephone: 46-46-2227415
Telefax: 46-46-2224427
www.byggnadsmaterial.lth.se

The Effect of Curing Conditions on Chloride Ingress in Concrete

Björn F. Johannesson

Lund Institute of Technology, Division of Building Materials

Box 118, SE-221 00 Lund, Sweden

Abstract

Concrete structures exposed to chlorides in, for example, marine environments or due to de-icing salting, suffer a considerable risk of being degraded due to reinforcement corrosion. Here, the effect of pre-curing conditions of concrete will be examined with respect to chloride ingress. Three different curing conditions and their effect on chloride ingress are studied. The different water to binder ratios tested are 0.35, 0.40 and 0.55. A sulfate-resistant Portland cement, SRPC, with 5 wt.% silica fume replacing cement was used. All samples tested were membrane-hardened one day after casting. The three different curing conditions tested were: direct exposure to sodium chloride, 1 week in tap water, and 2 weeks of drying in room climate followed by 1 week in tap water before exposure. A 3 wt.% sodium chloride outer storage solution was used for all tests. The total chloride profiles were measured by stepwise grinding of approximately 1.2 mm thick layers from the surface after 119 days of exposure using the rapid chloride test method, RCT. The hydration degree at the time of chloride exposure, the 7 day compressive strength and the active water-filled porosity was measured using capillary suction tests. The experimentally obtained chloride profiles were evaluated in three ways. The first consisted of measuring the depth at which the chloride content was 0.1 wt.% of concrete mass after 119 days of exposure. The second was a simple curve fitting using Fick's second law, to obtain the so-called effective diffusion constant. The last method is an approach taking into account the effect of different ions appearing in pore solution in terms of dielectrical effects, chemical binding and tortuosity in the pore system.

The conclusions drawn from the experiments are that 14 days of drying followed by 7 days of storage in tap water significantly increases the resistance to chloride penetration of concrete samples compared to samples, included in the tests, not dried before exposure. Furthermore, the difference of chloride penetration was found to be small for samples exposed directly to chlorides and samples stored in tap water for 7 days before exposure. From the method taking into account dielectrical effects the conclusion is drawn that the tortuosity factor for diffusion is smaller for samples dried in room climate before exposure. Furthermore, this method of evaluation of experimental data gave the result that samples dried before exposure to chloride had a greater ability to dissolve calcium and hydroxide from the solid constituents to the pore solution.

1 Introduction

The influence of the pre-curing of concrete samples before being exposed to a 3 wt.% sodium chloride solution is examined. The three studied pre-curing conditions all consisted of one-day membrane hardening after casting. A set of samples were exposed directly to the chloride solution after membrane hardening. Another set of samples were stored for 7 days in tap water before being exposed and the last set of samples were dried in room climate for 14 days and then rewetted in tap water for 7 days before being exposed to the chlorides. All samples were exposed for 119 days and were then removed from the bath and analyzed for total chloride content. The porosity of concrete samples was estimated either by calculations using the measured hydration degree at the time of exposure together with the cement content and the water to binder ratio of the mix, or by a direct method based on capillary suction of samples pre-dried in room climate. The 7 day compressive strength was also measured for the three tested concrete qualities.

A method which makes it possible to evaluate the effect of different ions diffusing in the pore solution has been developed. This method assumes that all different free ions dissolved in the pore solution are affected by the porosity and tortuosity of the material in an identical manner. The known measured diffusion coefficients for ions in bulk water are therefore scaled with the same tortuosity factor in order to account for the effect on the diffusion caused by the physical characteristics of the pore system. This way of treating the multi-component diffusion facilitates the introduction of effects

caused by electrostatic forces among different diffusing ions in pore solution. The assumptions for the mole density flow of the different ions are not only based on the mole density concentration gradient but also on the gradient of the electrostatic potential. This potential is calculated at each material point and at every time level using one of Maxwell's equations together with constitutive equations for the electrical displacement field vector and for the charge density scalar.

In the method described the active water-filled porosity, in which dissolved ions can appear, must be defined. The concentration of different ions in this representative part of the pore space serves as a state variable which is used when describing the interaction between dissolved ions and solid constituents at the pore walls, in terms of chemical reactions. Three types of chemical reactions are assumed, both equilibrium conditions and reaction kinetics are constituted. The binding of chlorides is dealt with by assuming that chloride ions are exchanged by substituting hydroxide in the solid calcium hydroxide structure to form calcium chloride. Dissolution of solid calcium hydroxide into the pore solution is dealt with and also dissolution of already formed solid calcium chloride.

The chloride binding and its dependence on pore solution alkalinity, CaO/SiO₂ ratio, cement type and C₃A content, cement fineness and water to cement ratio can be studied in [1]. In [2] it is concluded that bound chloride content of concrete decreases while the pH increases and that replacement of cement with silica fume reduces the chloride-binding capacity. The kinetics of chloride binding can be further studied in [3].

Once a relevant measure of the active porosity and the tortuosity factor for diffusion of dissolved ions in the pore system has been obtained, the problem of obtaining a proper model for chloride penetration very much shifts to the determination of the chemical reactions (or physical interaction) between ions in pore solution and solids at the pore walls.

Here it is assumed that the measured value of the total chloride content of samples collected 0-1.2 mm from the exposed surface, after 119 days of exposure, consists of a fraction being dissolved in the pore solution, and this concentration is the same as the outer storage chloride concentration; the rest of the ions are assumed to be bound into the solid structure. For simplicity the binding isotherm is assumed to be linear. That is, the whole chloride binding isotherm is given from the method described above.

The governed coupled equations for the considered ions in pore solution, i.e. in this case, Cl⁻, Na⁺, OH⁻, Ca²⁺, and K⁺, are established by

combining mass balance and charge balance equations together with constitutive equations, or equally material assumptions. These assumptions are tested by solving the whole set of coupled equations, with relevant boundary conditions, by using the finite element method. The material coefficients introduced, through the use of constitutive relations, are adjusted to give the best fit to the measured chloride concentration profiles. The obtained best fit values of these material constants are then judged by comparing their dependence on water to binder ratios and on the different curing conditions before exposure.

From experimental evidence alone it is concluded that a curing condition involving a drying period (followed by rewetting in tap water before exposure to chlorides) gives a lower ingress of chlorides compared to samples never dried before exposure. Further, for the types of conditions in the experiments performed, the drying process was shown to be of greater importance than the actual degree of hydration at the time of exposure.

The main conclusion drawn from simulations is that the composition of the pore solution in terms of different types of ions and their concentrations affects the chloride ingress. Furthermore, the condition of the storage solution is not only affected by its concentration of chloride ions, but also by other types of ions present. That is, the model established accounts for the effect of the composition of the storage solution on the chloride penetration into the material. The same type of conclusions have been drawn in [4], where chloride, sodium and calcium profiles were measured in concrete exposed to a chloride solution spray.

One interesting issue is that the experimentally obtained results show that the maximum concentration of chloride concentration in concrete, under certain conditions, is observed a few millimeters from the exposed surface even when samples are exposed to a constant outer concentration of chlorides, as is the case in all the experiments performed in this work. This phenomenon has been observed by other investigators, e.g. see [4]. The behavior could be modeled by taking into account dielectric effects among positive and negative ions in pore solution and also by taking into account for chemical reactions between solid hydration products and ions in pore solution.

Table 1: Diffusion coefficients and ionic mobilities for some ions in bulk water, at room temperature, [6] and [7].

Substance	Diffusion coeff. D (m ² /s)	Ionic mobility A (m ² /s/V)	Dielectricity coeff. $\epsilon\epsilon_o$ (C/V)
Cl ⁻	2.03·10 ⁻⁹	7.91·10 ⁻⁸	-
OH ⁻	5.30·10 ⁻⁹	20.64·10 ⁻⁸	-
Na ⁺	1.33·10 ⁻⁹	5.19·10 ⁻⁸	-
K ⁺	1.96·10 ⁻⁹	7.62·10 ⁻⁸	-
Ca ²⁺	0.79·10 ⁻⁹	6.17·10 ⁻⁸	-
H ₂ O	-	-	695.4·10 ⁻¹²

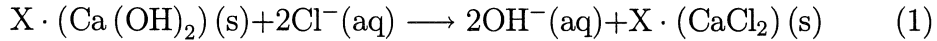
2 Governing equations

The equations to be presented here governing the diffusion and exchange of mass among the constituents are based on the so-called mixture theory, e.g. see [5]. The mass balance equations for the individual constituents are used together with the mass balance for the whole mixture. The constitutive equations consist of the description of the mass flow of ions and the chemical reaction rates and equilibrium conditions. The model includes five different ions dissolved in the pore solution: Cl⁻, Na⁺, OH⁻, Ca²⁺, and K⁺. Furthermore, two solid constituents are included, CaCl₂, and Ca(OH)₂; these two components are assumed to be incorporated in the hydration products of the cement.

The mass flow of ions are not solely described as being given by the concentration gradient but also as being dependent on the gradient of the electrostatic potential. This potential is a function of the composition of mixture. One of Maxwell's equations is used to calculate the electrostatic potential by applying constitutive equations for the electrical displacement field and the charge density scalar. When including the effect caused by the charge character of different ions on the diffusion behavior of each different ion type, it is important to include as many ions as possible appearing in pore solution, since the electrostatic potential is determined by the composition of the mixture of ions in solution.

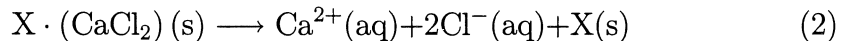
The chemical reaction describing binding of chlorides is assumed to be

caused by ion exchange as



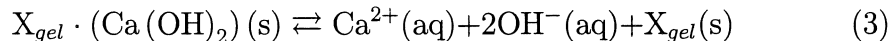
where the symbol X is included to stress that the crystalline calcium hydroxide is intergrown with the more or less amorphous hydration products of the cement. The effect that chlorides are bound, by chemical or/and physical forces, onto the micro-structure in cement-based materials has been experimentally observed by several researchers. The actual cause of this phenomenon has, however, been difficult to prove. Both the chemical formulation of Friedel's salt and the absorption of chlorides due to so-called physical binding have been proposed.

The second chemical reaction considered is dissolution of chloride ions from already formed calcium chloride involved in the hydration products. This reaction is written as



The inclusion of dissolution of chlorides in concrete becomes important when modeling cases where the outer exposure concentration of chlorides varies in a way that makes chlorides escape from the pore solution. This phenomenon will, most likely, affect the concentration of bound chlorides.

The third and last chemical reaction considered is dissolution of calcium hydroxide from the hydration products. The reaction is assumed to be reversible, as



In the following the different constituents will be denoted by numbers ranging from 1 to 7 as; Cl^- (1), Na^+ (2), OH^- (3), Ca^{2+} (4), K^+ (5), CaCl_2 (6), and $\text{Ca}(\text{OH})_2$ (7). The equations for the constituents will be expressed with the mole density concentration of ions related to the active water-filled porosity, denoted by n with a subscript indicating the type of ions referred to.

The description of the chloride ions dissolved in the pore solution, denoted by the subscript 1, is under the condition that the free concentration of chlorides is lower than or equal to the equilibrium concentration, expressed as $n_1^{eq} \leq n_1$, given as

$$\begin{aligned} \frac{\partial n_1}{\partial t} = & \text{div} \left(\tilde{D}_1 \text{grad} n_1 + \tilde{A}_1 v_1 n_1 \text{grad} \varphi \right) \\ & + R((K + Zn_3) n_6 - n_1) \end{aligned} \quad (4)$$

where $n_1^{eq} = (K + Zn_3)n_6$. The concentration n_1 , n_3 and n_6 denotes the mole density concentration of dissolved chlorides in pore solution, hydroxide ions in pore solution and solid calcium chloride, respectively, and φ denotes the electrostatical potential in pore solution. The first term on the right-hand side of (4) represents the effect of diffusion of chloride ions in pore solution and the last term $R((K + Zn_3)n_6 - n_1)$ represents binding of chloride. The diffusion coefficient \tilde{D}_1 and the ion mobility coefficient \tilde{A}_1 are formed by scaling the coefficients in bulk water, e.g. see Table 1, which includes values taken from [6] and [7], as $\tilde{D}_1 = tD_1$ and $\tilde{A}_1 = tA_1$, where t is the tortuosity factor, which is assumed to be the same for all different considered ions in the pore solution. The constant R expresses the kinetics of the binding of chlorides, according to the reaction (1), before reaching equilibrium, and K and Z are material constants determining the equilibrium binding isotherm. The property v_1 is the valence number for the chloride ion, i.e. $v_1 = -1$. If, for example, assuming the effect of hydroxide ion concentration in pore solution not affecting chloride binding, obtained by setting Z to zero, the equilibrium condition $n_1^{eq} = Kn_6$ is the so-called linear binding isotherm for chlorides. It is assumed that chloride binding is active whenever the actual concentration of chlorides in pore solution n_1 deviates from its equilibrium condition n_1^{eq} . The rate at which the binding occurs is assumed to be proportional to the ‘distance’ from equilibrium, i.e., by the term $n_1^{eq} - n_1$, by using the material constant R .

During cases when $n_1^{eq} > n_1$, i.e. when the concentration of bound chlorides is higher than its corresponding assumed equilibrium condition, in relation to the concentration of chlorides in pore solution, the rate constant R is replaced by S , in equation (4). The constant S denotes the rate of the dissolution of chlorides according to the reaction (2). It is assumed that the equilibrium conditions for reaction (1) and (2) are the same.

Sodium ions appearing dissolved in the pore solution, denoted by the subscript 2, are assumed not to be involved in any chemical reactions. The governed equation for this constituent, therefore, is obtained by combining mass balance and the constitutive relation for the mole density flow, to obtain

$$\frac{\partial n_2}{\partial t} = \text{div} \left(\tilde{D}_2 \text{grad} n_2 + \tilde{A}_2 v_2 n_2 \text{grad} \varphi \right) \quad (5)$$

where, again, the diffusion coefficient \tilde{D}_2 and the ion mobility coefficient \tilde{A}_2 , for the sodium ions, are obtained by scaling the corresponding bulk properties, given in Table 1, by the tortuosity factor t .

The hydroxide ions, dissolved in the pore solution, are under the condition $n_1^{eq} \leq n_1$, described as

$$\begin{aligned} \frac{\partial n_3}{\partial t} = & \operatorname{div} \left(\tilde{D}_3 \operatorname{grad} n_3 + \tilde{A}_3 v_3 n_3 \operatorname{grad} \varphi \right) \\ & - Q (W n_7 - n_3) - R ((K + Z n_3) n_6 - n_1) \end{aligned} \quad (6)$$

where hydroxide ions are supplied to pore solution by dissolution of hydroxide according to reaction (3), as described by the term $Q (W n_7 - n_3)$, where W describes the equilibrium isotherm and Q the kinetics of reaction, and due to supply of hydroxide according to reaction (1). Under conditions when $n_1^{eq} > n_1$ the material constant R is set to zero, since no supply of hydroxide ions to the pore solution exists during dissolution of chlorides according to reaction (2).

The mole density field of calcium ions in pore solution n_4 , under the condition $n_1^{eq} > n_1$, is determined by the following equation

$$\begin{aligned} \frac{\partial n_4}{\partial t} = & \operatorname{div} \left(\tilde{D}_4 \operatorname{grad} n_4 + \tilde{A}_4 v_4 n_4 \operatorname{grad} \varphi \right) \\ & - \frac{1}{2} Q (W n_7 - n_3) + \frac{1}{2} S ((K + Z n_3) n_6 - n_1) \end{aligned} \quad (7)$$

where the term $\frac{1}{2} Q (W n_7 - n_3)$ describes the rate of supply of calcium ions to pore solution due to reaction (3), and the term $\frac{1}{2} S ((K + Z n_3) n_6 - n_1)$ is the rate of reaction (2), contributing to production of calcium ions. When $n_1^{eq} = (K + Z n_3) n_6 \leq n_1$ the rate constant S is set to zero because the reaction described in (2) is not assumed to be active in this case.

The governed equation for the dissolved potassium ions in pore solution n_5 is

$$\frac{\partial n_5}{\partial t} = \operatorname{div} \left(\tilde{D}_5 \operatorname{grad} n_5 + \tilde{A}_5 v_5 n_5 \operatorname{grad} \varphi \right) \quad (8)$$

where, according to the reactions (1), (2) and (3), it is assumed that the potassium ions do not take place in any chemical reactions.

It will be explicitly assumed that the velocity of the solid CaCl_2 component is zero. That is, the differential equation describing the rate of change of the mole density of CaCl_2 is only due to the chemical reactions (1) or (2). If the condition $n_1^{eq} = (K + Z n_3) n_6 \leq n_1$ is the case, i.e. when reaction (1) is active, the governed equation for the solid calcium chloride is

$$\frac{\partial n_6}{\partial t} = -\frac{1}{2} R ((K + Z n_3) n_6 - n_1) \quad (9)$$

When $n_1^{eq} > n_1$, the rate constant R is replaced by the rate constant S for the reaction (2).

The solid calcium hydroxide constituent is assumed to have zero velocity. In conditions when $n_1^{eq} \leq n_1$ the description of the solid calcium hydroxide concentration n_7 is obtained by

$$\frac{\partial n_7}{\partial t} = \frac{1}{2}Q(Wn_7 - n_3) + \frac{1}{2}R((K + Zn_3)n_6 - n_1) \quad (10)$$

In situations when $n_1^{eq} > n_1$ the rate constant R is set to zero. The change of the concentration of solid calcium hydroxide is due to binding of chlorides according to reaction (1) and due to the dissolution of calcium hydroxide given by reaction (3).

The electrostatic potential φ , which is included in the equations for the diffusing dissolved ions in the pore solution, i.e. equations (4), (5), (6), (7) and (8), is an unknown property which must be calculated in order to account for the coupling of the constituent equations.

By using the static continuity equation for the charge together with the constitutive relations for the electric displacement field vector and the charge density, the governing equation for the static electro-potential becomes

$$-\text{div}(\tilde{\varepsilon}\varepsilon_0\text{grad}\varphi) = F \sum_{a=1}^5 n_a(\mathbf{x}, t) v_a, \quad (11)$$

where $\tilde{\varepsilon}\varepsilon_0$ is the dielectric coefficient for ions in pore solution and F is the Faraday's constant. The term on the right-hand side of (11) represents the charge imbalance, among the five different types of ions considered, being dissolved in pore water, at a certain material point and at a given time level.

Excluding the physical constant F , the model includes in total 17 material constants. The description of the velocity of the dissolved ions involves 5 diffusion constants and 5 ionic mobility constants; the description leading to a determination of the electrostatic potential involves one constant, i.e. the property $\tilde{\varepsilon}\varepsilon_0$; the description of the chemical equilibrium conditions involves 3 constants, i.e. K , Z and W ; and the description of the kinetics of the considered chemical reactions involves 3 rate constants, i.e. R , S and Q .

If motivated, the tortuosity factor t can be allowed to be dependent on the changes of the micro-structure caused by the chemical reactions assumed. i.e. (1), (2) and (3), and also on the degree of cement hydration. As will be shown later, a good match between experimentally obtained values and values

obtained from simulations, using the model described above, was obtained when having the tortuosity factor t independent of changes caused by the assumed chemical reactions and of the degree of cement hydration. Therefore, the tortuosity factor t must be seen as a mean value in this case, valid for a certain exposure time.

3 Experimental Procedure

Chloride profiles were measured for concretes based on three different water to binding ratios after 119 days of exposure to a 3 wt.% sodium chloride solution at room temperature. The concrete samples are based on a sulfate-resistant Portland cement, SRPC, trademark 'anläggningcement' and 5 wt.% silica fume replacing cement content, see Tables 2-5. Three different pre-curing conditions were used before exposure to chlorides. In total nine samples were tested. Three samples with water to binder ratios 0.35, 0.40 and 0.55 were exposed to the chloride solution one day after casting, and during this day of preparation the samples were membrane-hardened. The second considered preparation of the same concrete qualities consisted of one day of membrane-hardening, after casting, followed by one week of curing in tap water before exposure. The last set of samples were membrane-hardened after casting for one day followed by drying in room climate for two weeks and then rewetted in tap water for one week to prevent capillary suction of chloride-contaminated solution.

The concrete was cast in PVC cylinders with an inner diameter of 100 mm and a length of 180 mm. The concrete was vibrated on a table without obtaining water separation. The samples were sealed with plastic foil to prevent moisture exchange with the surrounding. After one day the plastic foil was removed and the samples were cut into one 60 mm thick disc and two 25 mm thick discs. The PVC-mould was kept around the periphery of the disc. One of the 25 mm thick discs was used to evaluate the hydration degree and the second 25 mm thick disc was used to evaluate the active porosity by performing a capillary suction test. The 60 mm disc was sealed with silicon in the joint between the PVC-mould and the concrete in order to assure a one-dimensional transport of chlorides once submerged into the sodium chloride solution.

A set of parallel samples, prepared in the same way as the samples being tested for chloride ingress, was analyzed for the degree of hydration, at the

time of exposure to chlorides. This test consisted of heating grained representative parts of samples to 105 °C and 1050 °C and measuring the loss of mass. At 105 °C the physically bound water is assumed to be lost and at 1050 °C the chemically bound water due to hydration is assumed lost. The loss on ignition at 1050 °C for the pure components were also measured and compensated for. After heating the samples were stored in an exsiccator in which the relative humidity was close to zero. When samples reached room temperature they were weighed.

The degree of hydration, α , for the different concretes was estimated from the measured weights using the following formula

$$\alpha = \frac{W_n}{C} = \frac{W_{105} \left(1 - \left(\frac{\mu_a + \Gamma \mu_c}{1 + \Gamma} \right) \right) - W_{1050}}{W_{1050} - \left(1 - \mu_a \right) \left(\frac{\Gamma}{1 + \Gamma} \right) W_{105}} \quad (12)$$

where W_n is the chemically bound water (kg), C is the weight of cement (kg), W_{105} is the weight after heating to equilibrium at 105 °C (kg), W_{1050} is the weight after heating to 1050 °C (kg), Γ is the ratio of gravel weight to cement weight, aggregate/cement (kg/kg), μ_a is the loss on ignition for gravel and pozzolans (kg/kg), μ_c is the loss on ignition for cement (kg/kg). The measured loss on ignition for the different components in concrete mix when heating to 1050 °C was: aggregate 0-8 mm 0.712%, aggregate 8-12 mm 0.250%, silica fume 1.304% and SRPC 0.689%. It should be noted that in expression 12 no special attention is paid to the hydration caused by the pozzolan reaction. A problem is that the long-term pozzolan reaction can result in water being gradually expelled from the hydration products, which is not accounted for in the proposed way of calculating the degree of hydration.

The 7 day compressive strength for cubic samples with sides 100 mm being stored in water, was measured using a standard compressive test. The values presented in Table 7, for the three examined concrete qualities, consists of the mean value of two tested cubes of each quality.

A capillary suction test was performed on samples dried in room climate for two weeks after the membrane hardening. The samples were allowed to suck water until the weight change was close to zero. The total amount of capillary sucked water serves as a measure of the active porosity. The initial water present in concrete before the capillary suction experiment started is not included in the active porosity measure. It is supposed to correspond to water hold in so narrow pores that it does not act as a 'vehicle' for chloride transport.

Samples never dried before exposure were analyzed for total porosity by using the measured values of the degree of hydration, at the time of exposure to chlorides, together with the cement content in mix. The formula $P_{tot} = C/1000(w/b - 0.19\alpha)$ is used, where C is the mass density concentration of cement in mix, w/b is the water to binder ratio and α is the degree of hydration.

After the three different preparations of specimens the 60 mm thick samples with its PVC-mould were submerged into a 3 wt.% sodium chloride solution. The solution was replaced twice during the 119 days of exposure.

Directly after the 119 days of exposure, approximately 1.2 mm thick layers were removed from the exposed surface by grinding. The concrete powder collected from each layer was stored in marked plastic bags. The depth from the exposed surface was measured with a slide-calliper at several locations before proceeding to the next layer. A mean value of the depth for each layer was used in defining the chloride profile.

The collected powder was analyzed for chloride content by using the rapid chloride test RCT. 1.5 ± 0.005 gram of the powder were stored in small bottles containing 10 ml of an acid dissolving the sample. The bottles were shaken for about 10 minutes before an ion selective electrode was inserted into the solution. The electrode was calibrated before and after use by performing tests on four chloride solutions with known compositions. The electrode was carefully washed before and after each measurement. The chloride content in powder is given by the reading from the electrode in terms of volts. The relation between the measured value and the chloride content is given from the calibration procedure. A calibration curve was established by fitting the measured result to the formula $C_{Cl} = a \exp(-bU)$, where a and b are the fitting parameters, U is the measured value in millivolts and C_{Cl} is the chloride content given as mass percent chlorides by concrete mass. The values obtained for a and b from the different calibrations are given in Tables 8-16.

In order to get an estimate of the accuracy of the rapid chloride test method a comparison was performed using titration with a CIBA-CORNING chloride analyzer. This method consists of a sample solution in contact with two electrodes. Silver ions are supplied from the silver anode by applying a constant current. When all chloride ions have been consumed by the silver ions the same ions increase rapidly in solution and a 'dead stop' function stops the current. The time period with the constant current applied to the solution serves as a measure of the number of dissolved chloride ions in test. It was found that the titration method systematically gave higher

Table 2: Mix proportions in concrete, SRPC with 5 percent silica replacing cement, water to binder ratio 0.55. Slump: 35 mm.

	Mass density (kg/m ³)	Weight in mix (kg)	Moisture (kg)
Cement	323	7.11	-
Silica	17	0.374	-
Aggregate 0-8 mm	966	21.33	0.0808
Aggregate 8-12 mm	857	18.85	-
Water	187	4.0332	-
Plasticizer	-	-	-

Table 3: Mix proportions in concrete, SRPC with 5 percent silica replacing cement, water to binder ratio 0.40. Slump: 50 mm.

	Mass density (kg/m ³)	Weight in mix (kg)	Moisture (kg)
Cement	399	8.78	-
Silica	21	0.462	-
Aggregate 0-8 mm	898	19.84	0.0790
Aggregate 8-12 mm	898	19.76	-
Water	168	3.5269	-
Plasticizer	6.3	0.1386	0.0901

values than the rapid chloride the test. From nine different comparisons the titrating procedure gave on average 9% higher values than the use of an ion selective electrode.

Experimental data on the composition of the pore solution, for a 5-month-old concrete stored in water produced with SRPC, described in Table 5, with a water to binder ratio of 0.40 with 5 wt.% silica fume replacing cement, are presented in Table 17. The experiment was performed by the Swedish research laboratory EUROCC RESEARCH. The water in concrete was drained by applying a pressure to the sample. The potassium and sodium ions were detected with IPC-analyses and the hydroxide ions using titration. The values in Table 17 will be used as a quantitative measure of the condition of the pore solution in concrete, at the time of exposure to a sodium chloride solution.

Table 4: Mix proportions in concret, SRPC with 5 percent silica replacing cement, water to binder ratio 0.35. Slump: 30 mm

	Mass density (kg/m ³)	Weight in mix (kg)	Moisture (kg)
Cement	427.5	9.40	-
Silica	22.5	0.495	-
Aggregate 0-8 mm	858	18.95	0.0717
Aggregate 8-12 mm	929	20.44	-
Water	157.5	3.2646	-
Plasticizer	9	0.198	0.1287

Table 5: Typical composition of examined cement and pozzolan used.

Component	Composition SRPC (Percent of total)	Composition silica (Percent of total)
CaO	63.8	0.4
SiO ₂	22.8	94.2 (amorphous)
Al ₂ O ₃	3.48	0.62
Fe ₂ O ₃	4.74	0.95
MgO	0.80	0.65
SO ₃	1.88	0.33
K ₂ O	0.55	0.5
Na ₂ O	0.06	0.2
Ignition loss	0.72	1.8

Table 6: Measured porosities based on capillary water uptake and calculated total porosities at the time of exposure to chlorides. The different preconditions are: (a) two weeks of drying in room climate followed by one week's storage in tap water, (b) one week of storage in tap water, (c) one day membrane hardening.

Concrete (w/b)	Active porosity (a) (m^3/m^3)	Calc. tot. porosity (b) (m^3/m^3)	Calc. tot. porosity (c) (m^3/m^3)
0.35	0.0562	0.104	0.1204
0.40	0.0788	0.118	0.1323
0.55	0.1073	0.142	0.1537

Table 7: Degree of hydration at the time of exposure. The different preconditions are: (a) two weeks of drying in room climate followed by one week's storage in tap water, (b) one week of storage in tap water, (c) one day membrane hardening.

Concrete (w/b)	Degree of hydration (-)	Comp. strength (7 days) (MPa)
0.35 (a)	0.56	77
0.40 (a)	0.55	66
0.55 (a)	0.58	39
0.35 (b)	0.59	77
0.40 (b)	0.55	66
0.55 (b)	0.56	39
0.35 (c)	0.36	77
0.40 (c)	0.36	66
0.55 (c)	0.39	39

Table 8: Total chloride profile, water to binder ratio 0.55. Sample dried for two weeks followed by one week's storage in tap water before exposure to a 3 weight percent sodium chloride solution for 119 days. Calibration constants: $a = 0.4283$ and $b = 0.04238$, see section 3.

Depth (mm)	U (mV)	Total Cl ⁻ (wt.% of concrete)
0.0-1.0	22.8	0.163
1.0-2.0	19.4	0.188
2.0-2.9	20.6	0.179
2.9-4.1	20.9	0.177
4.1-5.1	22.4	0.166
6.6-8.5	32.1	0.110
10.7-12.3	46.9	0.059
16.1-17.5	78.4	0.015
21.9-23.7	118.6	0.003
27.0-29.6	120.9	0.003

Table 9: Total chloride profile, water to binder ratio 0.40. Sample dried for two weeks followed by one week's storage in tap water before exposure to a 3 weight percent sodium chloride solution for 119 days. Calibration constants: $a = 0.4283$ and $b = 0.04238$, see section 3.

Depth (mm)	U (mV)	Total Cl ⁻ (wt.% of concrete)
0.0-0.09	19.0	0.191
0.09-1.8	14.1	0.236
1.8-2.6	13.9	0.238
2.6-4.0	15.2	0.225
4.0-6.0	19.8	0.185
6.0-7.5	27.6	0.133
10.1-11.0	60.7	0.033
15.1-16.5	116.6	0.003
22.1-24.3	120.9	0.003
28.9-30.2	121.1	0.003

Table 10: Total chloride profile, water to binder ratio 0.35. Sample dried for two weeks followed by one week's storage in tap water before exposure to a 3 weight percent sodium chloride solution for 119 days. Calibration constants: $a = 0.4270$ and $b = 0.04154$, see section 3.

Depth (mm)	U (mV)	Total Cl ⁻ (wt.% of concrete)
0.0-1.0	15.7	0.222
1.0-2.0	12.1	0.258
2.0-2.9	12.6	0.253
2.9-5.0	18.4	0.199
5.0-5.9	30.5	0.120
8.8-9.8	68.1	0.025
12.1-13.6	103.2	0.006
17.7-19.8	125.3	0.002
26.6-29.1	126.5	0.002

Table 11: Total chloride profile, water to binder ratio 0.55. Sample stored for one week in tap water before exposure to a 3 weight percent sodium chloride solution for 119 days. Calibration constants: $a = 0.4184$ and $b = 0.04191$, see section 3.

Depth (mm)	U (mV)	Total Cl ⁻ (wt.% of concrete)
0.0-1.8	-9.0	0.610
1.8-2.5	-5.3	0.522
2.5-3.7	-3.0	0.474
7.1-9.0	15.0	0.223
13.0-14.6	38.7	0.083
19.2-20.7	63.3	0.029
26.0-30.5	109.0	0.004

Table 12: Total chloride profile, water to binder ratio 0.40. Sample stored for one week in tap water before exposure to a 3 weight percent sodium chloride solution for 119 days. Calibration constants: $a = 0.4298$ and $b = 0.04157$, see section 3.

Depth (mm)	U (mV)	Total Cl ⁻ (wt.% of concrete)
0.0-1.2	-2.8	0.483
1.2-2.1	-1.1	0.450
2.1-3.6	1.2	0.409
3.8-5.5	12.0	0.261
5.9-6.5	15.6	0.225
6.5-8.1	20.0	0.187
12.5-14.1	53.2	0.047
18.3-19.8	107.4	0.005
23.9-26.6	118.2	0.003
26.6-30.0	119.9	0.003

Table 13: Total chloride profile, water to binder ratio 0.35. Sample stored for one week in tap water before exposure to a 3 weight percent sodium chloride solution for 119 days. Calibration constants: $a = 0.4184$ and $b = 0.04191$, see section 3.

Depth (mm)	U (mV)	Total Cl ⁻ (wt.% of concrete)
0.0-1.2	-4.6	0.507
1.2-3.0	-0.1	0.420
3.0-4.8	6.7	0.316
7.2-8.5	27.7	0.131
11.7-13.7	83.1	0.013
17.2-19.2	119.0	0.003
23.6-26.1	121.6	0.003
26.1-28.8	118.8	0.003

Table 14: Total chloride profile, water to binder ratio 0.55. Sample membrane-hardened for one day before exposure to a 3 weight percent sodium chloride solution for 119 days. Calibration constants: $a = 0.4196$ and $b = 0.04232$, see section 3.

Depth (mm)	U (mV)	Total Cl ⁻ (wt.% of concrete)
0.0-1.1	-4.3	0.503
1.1-2.1	-8.5	0.601
2.1-3.9	-3.3	0.482
3.9-5.0	3.4	0.363
9.4-10.3	18.1	0.195
13.4-14.8	36.5	0.090
19.3-21.1	57.9	0.036
24.3-26.0	83.3	0.012
27.6-29.8	108.3	0.004

Table 15: Total chloride profile, water to binder ratio 0.40. Sample membrane-hardened for one day before exposure to a 3 weight percent sodium chloride solution for 119 days. Calibration constants: $a = 0.4196$ and $b = 0.04232$, see section 3.

Depth (mm)	U (mV)	Total Cl ⁻ (wt.% of concrete)
0.0-1.4	-5.6	0.532
1.4-2.2	-6.9	0.562
2.2-3.4	-3.4	0.491
5.3-6.2	9.3	0.283
9.4-10.6	27.7	0.130
15.0-16.2	67.7	0.024
19.6-20.7	106.8	0.005
24.2-26.2	114.3	0.003
26.2-28.9	111.1	0.004
28.9-30.7	118.5	0.003

Table 16: Total chloride profile, water to binder ratio 0.35. Sample membrane-hardened for one day before exposure to a 3 weight percent sodium chloride solution for 119 days. Calibration constants: $a = 0.4180$ and $b = 0.04199$, see section 3.

Depth (mm)	U (mV)	Total Cl ⁻ (wt.% of concrete)
0.0-0.8	-2.4	0.462
0.8-1.7	0.1	0.416
1.7-2.6	5.4	0.333
2.6-5.7	11.2	0.261
7.0-8.4	25.5	0.143
8.6-10.0	35.8	0.093
10.0-12.3	48.6	0.054
16.8-19.6	110.6	0.004
25.3-30.2	123.4	0.002

Table 17: Pore extraction data for concrete. Cement as described in Table 5, water to binder ratio 0.40, 5 weight percent silica fume replacing cement content

Material	K ⁺ (mmol/l)	Na ⁺ (mmol/l)	OH ⁻ (mmol/l)	(Error)
w/b 0.40	255	34	286	3

4 Simulation of chloride ingress

Simulation of chloride ingress will be performed using the model described in section 2. The diffusion of the five different types of ions considered here is assumed to take place in the pore solution the volume of which is defined by the active porosity, see Table 6, and the diffusion coefficient and the ion mobility coefficient in bulk water are assumed to be used together with a scaling constant t , accounting for tortuosity of the pore system.

The interaction of diffusing negative and positive ions is treated by calculating the electrostatic potential, whose gradient will affect the diffusion of the individual types of ions in a way that the electron neutrality is very close to zero at every material point and at every time level.

The finite element method, e.g. see [8], [9] and [10], is used to solve the set of coupled equations described in section 2. Simple linear one-dimensional elements are used. The time integration adopted is an implicit one-step method referred to as the Liniger algorithm. The damping and stiffness matrix are established for the whole equation system including all constituents. Therefore, the concentration fields of the different constituents are calculated at one step only at every time level. The coupling terms appear as off-diagonal terms in the global stiffness matrix. The off-diagonal terms are due to chemical reactions and dielectrical effects among the positive and negative ions in pore solution. The material non-linearities are caused by the introduction of the dielectrical effects. The numerical treatment of these non-linearities is simply tackled by using small time steps and by evaluating the parameters explicitly at each time level. A test where the time steps are gradually decreased was performed to check at which time step lengths the solutions were no longer affected.

The initial conditions in terms of mole concentrations of ions in pore solution for K^+ , Na^+ , OH^- and Ca^+ are set to 255, 31, 306 and 10 (mol/m^3), which are in the range corresponding to the measured values given in Table 17. The outer concentration of sodium and chloride ions is set to 510 (mol/m^3), which corresponds to the conditions in the experiments with which the test results are to be compared.

The boundary condition used for the equation solving the electrostatic field is a description of the potential at the exposed surface. This potential is set to zero at the surface because the net charge density of the mixture of ions at this point is zero. This is due to the application of boundary conditions, in terms of mole density concentrations, whose composition is always neutral

with respect to the ionic charge.

The domain of interest is treated as a one-dimensional problem which is divided into two symmetrical parts. This becomes possible due to the symmetrical geometry and due to the symmetry in the applied boundary conditions. The studied total length of the one-dimensional domain in this simulation is 30 mm.

The material constants used to fit the experimental data are the tortuosity factor t , the binding capacity of chlorides $1/K$ and the dissolution rate of hydroxide, described with the material constant Q together with the description of the equilibrium condition using the constant W . The binding rate of chlorides, described by the constant R , is set to the same value for all three concrete qualities and for all curing conditions.

It should be noted that the diffusion coefficients and ion mobility coefficients in bulk water, given in Table 1, are used together with the same tortuosity factor t for all ions. This implies that different dissolved ions are affected by the geometry of the pore system in the same manner. Another important measure is the porosity which either is given by the measured active water-filled porosity based on capillary suction tests or by the calculated total porosity, given by considering the degree of hydration, water to binder ratio and cement content in mix, see Table 6. Dissolved ions appearing in the material are assumed to be spread out in the active water-filled porosity.

The binding rate of chlorides R and the binding capacity of hydroxide ions W are set to 0.0012 (1/s) and 0.0102 (-), respectively, for all different simulations on the different concrete qualities and curing conditions. Further, the coefficient of permittivity $\tilde{\epsilon}\epsilon_0$ is set to $6.95 \cdot 10^{-10}$ (C/V) which is the value valid for bulk water at 25°C. The influence on chloride binding caused by different hydroxide ion concentrations in pore solution is assumed to be negligible by setting the material constant Z to zero.

The coupling of the governed equations for the ion constituents in the model to be tested is crucial. Therefore, the determination of all concentration fields of the constituents is important since they will affect the chloride penetration. The results shown are, however, only in terms of total chloride profiles which can be compared with the measurements presented in section 3.

In Figures 1-3 the results of the simulation in terms of total chloride profiles, after 119 days of exposure, are shown (solid line). These results are for samples dried in room climate for two weeks and rewetted in tap water for one week before exposure to a constant 3 wt.% sodium chloride solution.

The measured values for all tests, see Tables 8-16, are given as percentage of chloride mass by concrete mass. These values are converted to a mole density concentration of chlorides related to the active pore volume given from the capillary suction experiments or from the calculated total porosity.

In order to show the influence of including dielectrical effects among the positive and negative ions in pore solution, a parallel simulation was performed where the ion mobilities for all considered dissolved ion constituents were set to zero. These results are presented as dashed lines in Figures 1-9.

The converted measured values and simulations for samples stored for one week in tap water before exposure to chlorides are presented in Figures 4-6. The effects caused by the dielectrical interaction among the different dissolved ions is for this case smaller than the samples dried for two weeks and rewetted one week before exposure, e.g. compare Figures 1-3 with Figures 4-6.

In Figures 7-9, the comparison of measurements and simulation for the samples directly exposed to chlorides after one day of membrane hardening after casting. The match is poorer for the water to binder ratios 0.40 and 0.55 for this type of pre-curing of samples compared to others. This is because the binding rate constant of hydroxide for all three concrete qualities with this preparation had the same value. A better match between measurements and simulations would, in this case, easily be obtained if one allowed for the used of different binding rate constants of hydroxide for the different water to binder ratios.

5 Results of simulations

Three methods of evaluating the effect of the pre-curing condition on chloride ingress into concrete are examined. The first is simply to check at which depth the chloride concentration is 0.1% of concrete mass after 119 days of exposure. This depth was obtained by linear interpolation of the measured values presented in Tables 8-16. The second approach is the 'classical' method of fitting the solution of Fick's second law to the measured total chloride concentration profiles, shown in Tables 8-16. This method leads to the determination of the so-called effective diffusion coefficient. No special attention is paid to the applied boundary conditions, non-linear binding and interaction of different ion constituents in this approach. The last method of evaluating the measured chloride profiles is to study the values of the material parameters giving the best fit to measured data using the proposed model

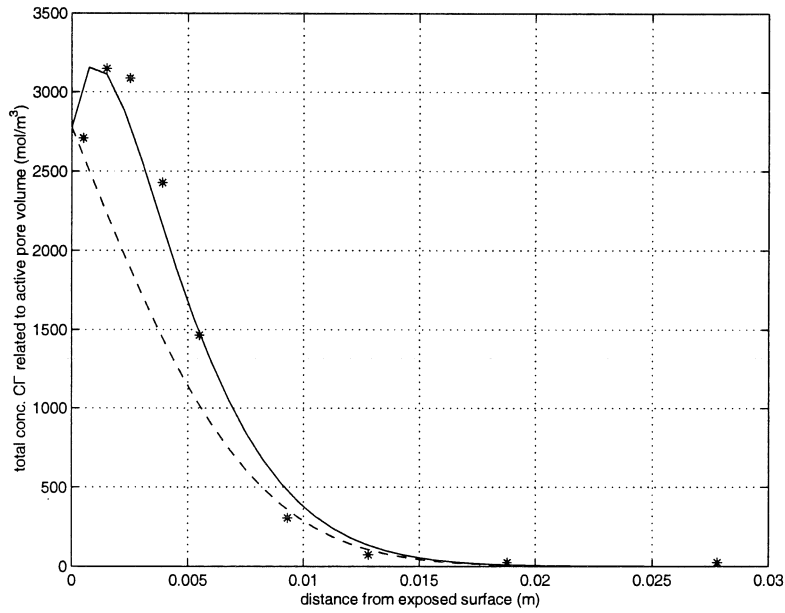


Figure 1: Results for the SRPC concrete with 5 wt.% silica fume replacing cement, water to binder ratio 0.35. Total concentration of chloride ions in relation to the active pore volume after 119 days of exposure to a 3 wt.% sodium chloride solution. Samples were dried for two weeks and rewetted for one week before exposure to chlorides. The stars represent measured values. The dashed line is the result of the simulation when not taking into account dielectrical effects and the solid line is the case when dielectrical effects are considered.

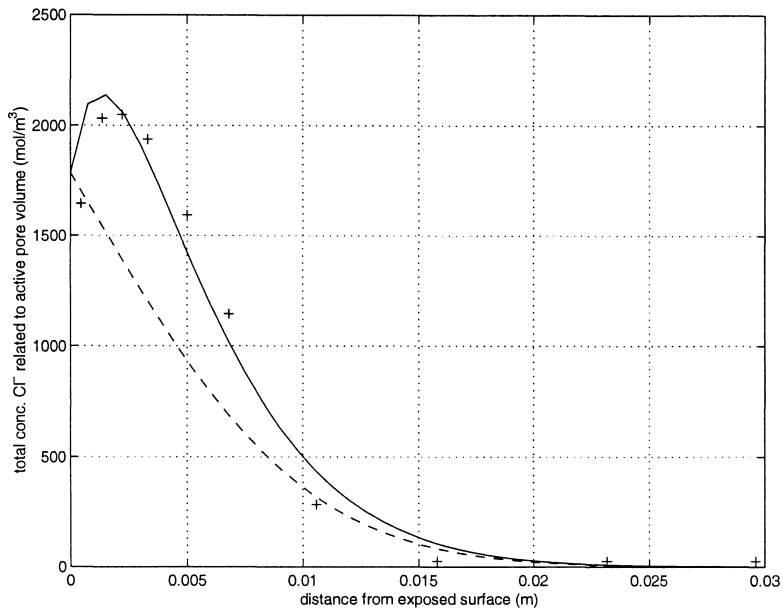


Figure 2: Results for the SRPC concrete with 5 wt.% silica fume replacing cement, water to binder ratio 0.40. Total concentration of chloride ions in relation to the active pore volume after 119 days of exposure to a 3 wt % sodium chloride solution. Samples were dried for two weeks and rewetted for one week before exposure to chlorides. The stars represent measured values. The dashed line is the result of the simulation when not taking into account dielectrical effects and the solid line is the case when dielectrical effects are considered.

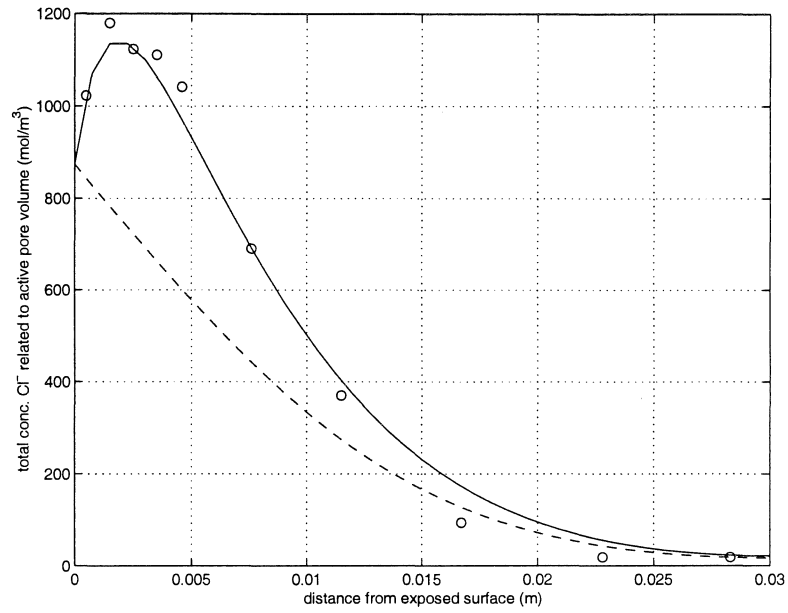


Figure 3: Results for the SRPC concrete with 5 wt.% silica fume replacing cement, water to binder ratio 0.55. Total concentration of chloride ions in relation to the active pore volume after 119 days of exposure to a 3 wt.% sodium chloride solution. Samples were dried for two weeks and rewetted for one week before exposure to chlorides. The stars represent measured values. The dashed line is the result of the simulation when not taking into account dielectrical effects and the solid line is the case when dielectrical effects are considered.

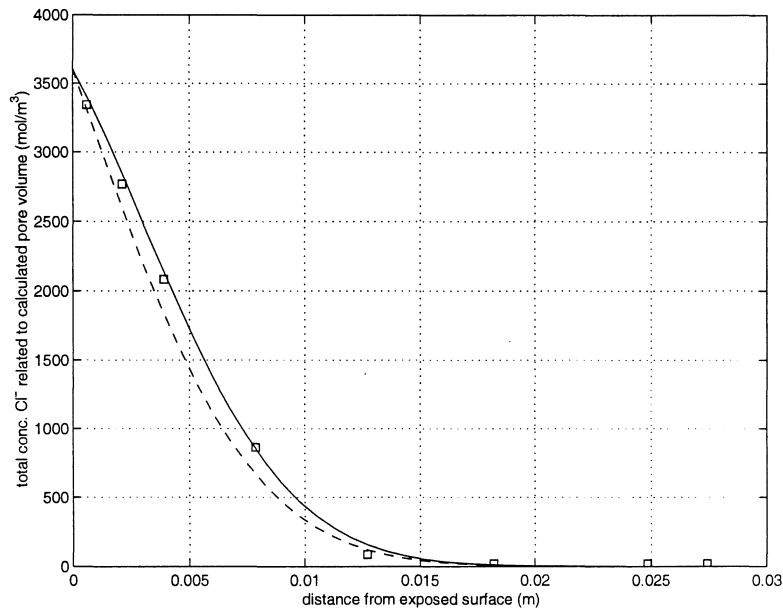


Figure 4: Results for the SRPC concrete with 5 wt.% silica fume replacing cement, water to binder ratio 0.35. Total concentration of chloride ions, in relation to the calculated pore volume, after 119 days of exposure to a 3 wt.% sodium chloride solution. Samples were stored for one week in tap water before exposure to chlorides. The stars represent measured values. The dashed line is the result of the simulation when not taking into account dielectrical effects and the solid line is the case when dielectrical effects are considered.

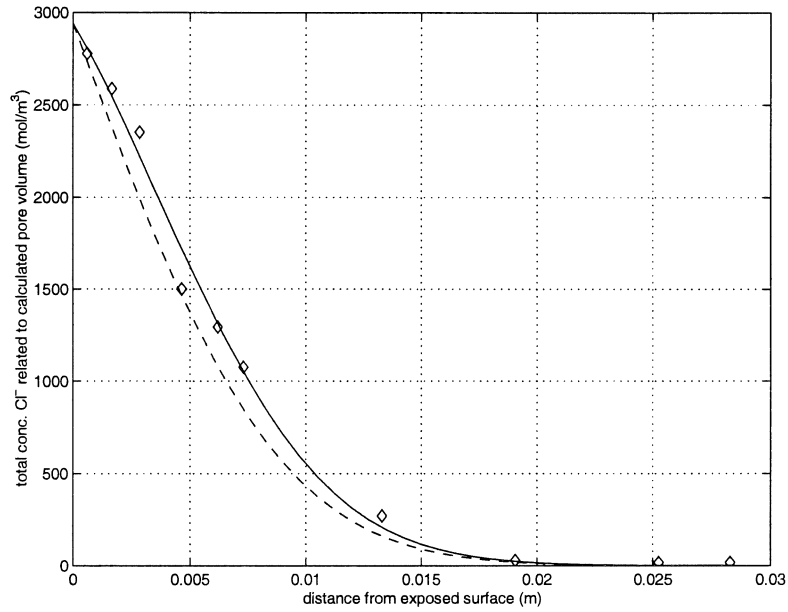


Figure 5: Results for the SRPC concrete with 5 wt.% silica fume replacing cement, water to binder ratio 0.40. Total concentration of chloride ions, in relation to the calculated pore volume, after 119 days of exposure to a 3 wt.% sodium chloride solution. Samples were stored for one week in tap water before exposure to chlorides. The stars represent measured values. The dashed line is the result of the simulation when not taking into account dielectrical effects and the solid line is the case when dielectrical effects are considered.

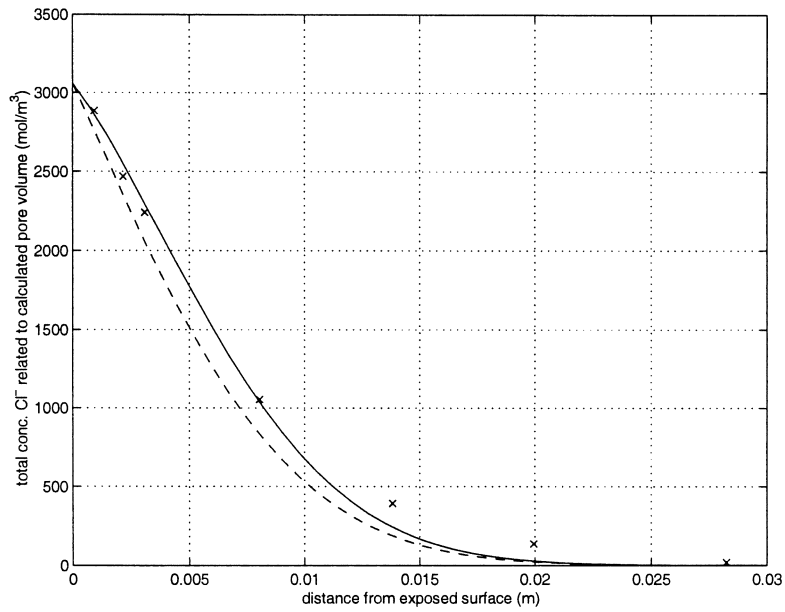


Figure 6: Results for the SRPC concrete with 5 wt.% silica fume replacing cement, water to binder ratio 0.55. Total concentration of chloride ions, in relation to the calculated pore volume after 119 days of exposure to a 3 wt.% sodium chloride solution. Samples were stored for one week in tap water before exposure to chlorides. The stars represent measured values. The dashed line is the result of the simulation when not taking into account dielectrical effects and the solid line is the case when dielectrical effects are considered.

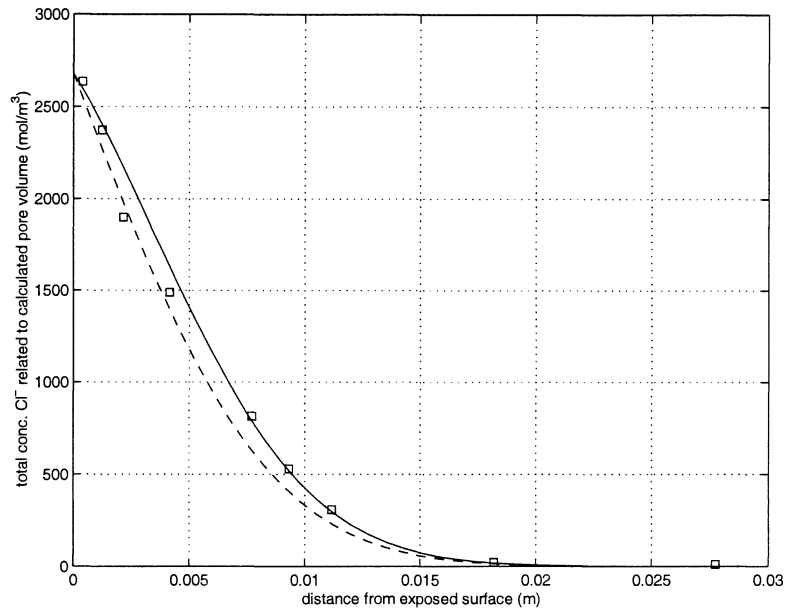


Figure 7: Results for the SRPC concrete with 5 wt.% silica fume replacing cement, water to binder ratio 0.35. Total concentration of chloride ions, in relation to the calculated pore volume after 119 days of exposure to a 3 wt.% sodium chloride solution. Samples were membrane-hardened for one day before exposure to chlorides. The stars represent measured values. The dashed line is the result of the simulation when not taking into account dielectrical effects and the solid line is the case when dielectrical effects are considered.

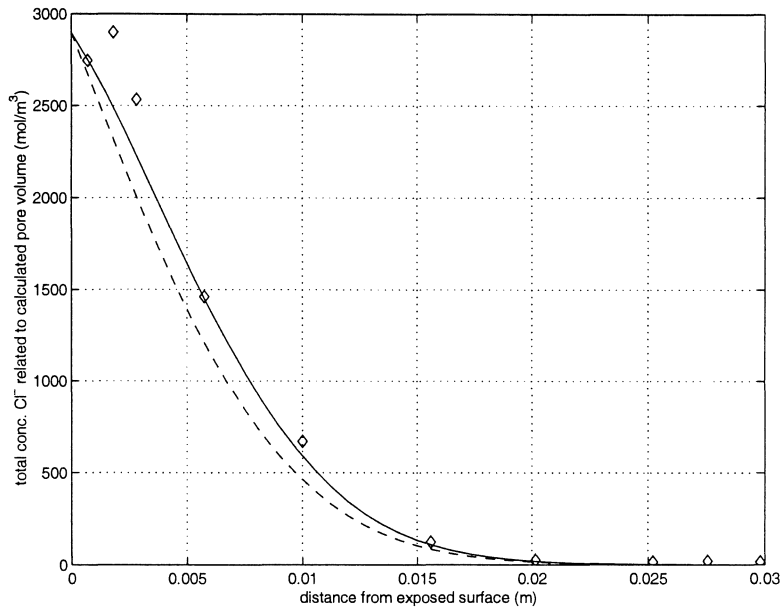


Figure 8: Results for the SRPC concrete with 5 wt.% silica fume replacing cement, water to binder ratio 0.40. Total concentration of chloride ions, in relation to the calculated pore volume after 119 days of exposure to a 3 wt.% sodium chloride solution. Samples were membrane-hardened for one day before exposure to chlorides. The stars represent measured values. The dashed line is the result of the simulation when not taking into account dielectrical effects and the solid line is the case when dielectrical effects are considered.

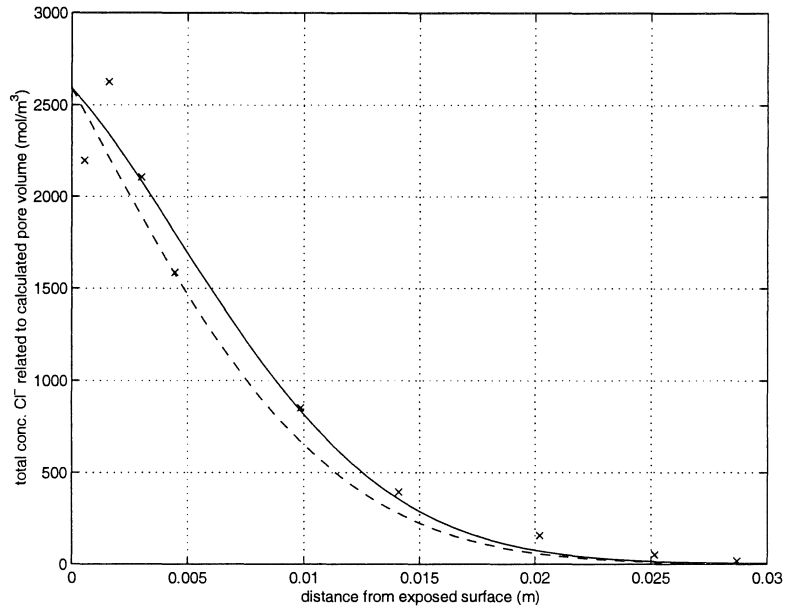


Figure 9: Results for the SRPC concrete with 5 wt.% silica fume replacing cement, water to binder ratio 0.55. Total concentration of chloride ions, in relation to the calculated pore volume after 119 days of exposure to a 3 wt.% sodium chloride solution. Samples were membrane-hardened for one day before exposure to chlorides. The stars represent measured values. The dashed line is the result of the simulation when not taking into account dielectrical effects and the solid line is the case when dielectrical effects are considered.

Table 18: Material constants, giving the best fit between the calculated chloride profile and the measured chloride profiles, for the three different concrete mixes dried for two weeks and rewetted for one week before exposure to a 3 weight percent sodium chloride solution.

Material constants	w/b 0.35	w/b 0.40	w/b 0.55
Tortuosity factor, t (-)	0.00516	0.00550	0.00561
Binding cap., Cl^- , $1/K$ (-)	2.22	1.25	0.36
Binding rate Cl^- , R (1/s)	0.0012	0.0012	0.0012
Binding cap., OH^- , W (-)	0.0102	0.0102	0.0102
Binding rate, OH^- , Q (1/s)	$1 \cdot 10^{-6}$	$1 \cdot 10^{-6}$	$1 \cdot 10^{-6}$
Measured active porosity	0.0562	0.0788	0.1073

described in section 2.

All three evaluation methods gave the result that pre-conditioning consisting of two weeks of drying followed by wetting in tap water for one week, before exposure, gives the lowest penetration depths of the three studied pre-curing cases.

The results obtained from the simulation using the model described in section 2 are given in terms of, (i) the tortuosity factor t , which is the same for all dissolved ions presented in a certain pore system, (ii) the binding capacity of chlorides and (iii) the binding rate of hydroxide ions. Only two different values of the binding rate are adopted for hydroxide ions in pore solution. For the pre-curing consisting of two weeks of drying followed by rewetting for one week before exposure to chlorides the value $-1 \cdot 10^{-6}$ (1/s) was used. For the two other pre-curing conditions the value $-2 \cdot 10^{-7}$ (1/s) was used. This did, indeed, result in a somewhat poor match for two of the performed test, e.g. compare Figures 8 and 9.

In order to obtain a quantitative comparison between the evaluation method leading to the effective diffusion constant D_{eff} and the model described in section 2, an effective diffusion constant, denoted D_{eff}^* , will be formed as: $D_{eff}^* = \tilde{D}_1 / (1 + 2K^{-1})$, where \tilde{D}_1 is the scaled bulk diffusion coefficient for chlorides in the pore system and K^{-1} is the binding capacity of chlorides. The reason for using this relation is based on combining a diffusion equation, given as $\partial \rho_{cl} / \partial t = \tilde{D}_1 \partial^2 \rho_{cl} / \partial x^2 - \partial \rho_{cl}^b / \partial t$, where $-\partial \rho_{cl}^b / \partial t$ is the mass exchange rate between dissolved chlorides in pore solution and bound chlorides, with an equilibrium binding isotherm relation given as: $\rho_{cl}^b =$

Table 19: Material constants, giving the best fit between the calculated chloride profile and the measured chloride profiles, for the three different concrete mixes stored in water for one week before exposure to 3 weight percent sodium chloride solution.

Material constants	w/b 0.35	w/b 0.40	w/b 0.55
Tortuosity factor, t (-)	0.00619	0.00682	0.00805
Binding cap., Cl^- , $1/K$ (-)	3.03	2.38	2.50
Binding rate Cl^- , R (1/s)	0.0012	0.0012	0.0012
Binding cap., OH^- , W (-)	0.0102	0.0102	0.0102
Binding rate, OH^- , Q (1/s)	$2 \cdot 10^{-7}$	$2 \cdot 10^{-7}$	$2 \cdot 10^{-7}$
Calculated porosity	0.104	0.118	0.142

$2K^{-1}\rho_{cl}$, where ρ_{cl}^b and ρ_{cl} are the mass density concentrations of bound and free chlorides, respectively. The diffusion equation and the binding isotherm together combine to the equation, $\partial\rho_{cl}/\partial t = \tilde{D}_1/(1 + 2K^{-1})\partial^2\rho_{cl}/\partial x^2$. It is seen that a high binding capacity reduces the penetration of chlorides since D_{eff}^* , in this case, becomes small. The equilibrium binding isotherm $\rho_{cl}^b = 2K^{-1}\rho_{cl}$ corresponds to the equilibrium condition used in the model described in section 2, when setting $Z = 0$, i.e. $n_1^{eq} = Kn_6$. The factor 2 used in $\rho_{cl}^b = 2K^{-1}\rho_{cl}$ is due to this relation being expressed in terms of mass density concentrations and the relation $n_1^{eq} = Kn_6$ in mole density concentrations.

It should be carefully noted that the estimated effective diffusion constant D_{eff}^* does not account for interaction between ions caused by dielectrical effects nor does it consider non-linear binding of chlorides. Therefore, calculations based on D_{eff}^* should correspond fairly well to the chloride profiles shown as dashed lines in Figures 1-9. Furthermore, when not having a significant increase of chloride concentration near the exposed surface, as was the case in the experiments presented in Figures 4-7, the values of D_{eff}^* are expected to be significantly smaller than the D_{eff} values, e.g. compare Table 21.

The numerical simulations shows that the tortuosity factor increases and the binding capacity decreases when the water to binder ratio increases when comparing concretes subjected to the same pre-curing conditions. It is further observed that the differences between the tortuosity factor are small and the differences in binding capacities of chloride ions are great between the three water to binder ratios tested, when samples are dried before exposure, see

table 18, compared to when the samples are undried before exposure, see Table 19 and 20. This may be due to the change of the micro-structure of the concrete when subjected to drying at early ages. According to the results from the simulation, the drying process, before the exposure to chlorides, makes the micro-structure less sensitive to different water to binder ratio as regards the diffusion in the pore system. On the other hand, the binding capacity of chlorides is greatly affected by the water to binder ratio in this case.

In [11] tortuosity factors for concrete are determined by a gas diffusion technique. The tortuosity factors obtained for concrete with the cement content 400 kg/m^3 having water to cement ratios 0.40 and 0.55 were 0.007 and 0.011, respectively. These values are in good agreement with the ones obtained in this study, for samples never dried before exposure, i.e. see Tables 19 and 20. A theoretical concepts involving tortuosity factors using the so-called homogenization technique has been suggested. This method has been applied to ion diffusion in cement-based materials, e.g. see [12].

Another result obtained by fitting simulated chloride profiles to measured values is that the difference between tortuosity factors and binding capacities for chlorides for samples exposed directly to chlorides, and for samples stored in tap water for one week before exposure, is relatively small, compare values given in Tables 19 and 20. This is most likely due to the proceeding hydration of samples during the chloride penetration tests. The results, in terms of tortuosity and binding capacity, from samples dried for two weeks and rewetted in tap water for one week before exposure, indicates that proceeding hydration during tests cannot compensate for the micro structural changes caused by drying.

It is of great importance to note that the material constants associated with penetration of chloride ions, i.e. the diffusion coefficient, the tortuosity factor, the binding capacity and the binding rate for chloride, cannot alone give a measure of the condition of chloride penetration resistance for a certain tested concrete. It is also the combination of different types of ions in pore solution and their corresponding diffusion coefficients, and constants describing reactions involving these ions, which will affect the penetration. This is due to dielectrical effects and chemical reactions among constituents in the mixture. Further, the condition of the storage solution, in terms of concentration of different ions, will affect the penetration of chlorides in the studied model. This can, for example, be the case when the outer storage solution has a high hydroxide ion concentration which will hinder the leach-

Table 20: Material constants, giving the best fit between the calculated chloride profile and the measured chloride profiles, for the three different concrete mixes exposed to a 3 weight percent sodium chloride solution after one day of membrane hardening.

Material constants	w/b 0.35	w/b 0.40	w/b 0.55
Tortuosity factor, t (-)	0.00550	0.00715	0.00962
Binding cap., Cl^- , $1/K$ (-)	2.13	2.34	2.04
Binding rate Cl^- , R (1/s)	0.0012	0.0012	0.0012
Binding cap., OH^- , W (-)	0.0102	0.0102	0.0102
Binding rate, OH^- , Q (1/s)	$2 \cdot 10^{-7}$	$2 \cdot 10^{-7}$	$2 \cdot 10^{-7}$
Calculated porosity	0.1204	0.1323	0.1537

ing of hydroxide from the pore solution. The dissolution of solid calcium hydroxide will therefore be small. The electrical equilibration process among positive and negative ions in pore solution, in such a case, will be very different from a case where a pure sodium chloride solution is used as outer storage condition. The model described in section 2 is developed in a way that all these effects can be studied in a stringent and systematic manner.

6 Conclusions

From the chloride penetration experiments it was seen that a pre-curing before exposure to chloride consisting of two weeks of drying followed by one week submerged in tap water significantly reduced the ingress of chloride compared to samples that were exposed directly to a chloride solution or stored for one week in tap water before exposure. The difference in terms of chloride ingress for samples exposed directly to chlorides and samples stored for one week in tap water before exposure was, however, shown to be small. The above results were independent of the water to binder ratio.

From the simulation of chloride penetration it is concluded that one possible explanation for the observed maximum in chloride content a few millimeters from the exposed surface is a combined effect of leaching of hydroxide ions from solid hydration products and dielectrical effects among different types of ions dissolved in pore solution. According to the simulation the maximum in chloride content a few millimeters from the exposed surface becomes significant after approximately two months of exposure, which is due to

Table 21: Comparison between chloride transport coefficients valid for different curing conditions. The different pre-conditions before chloride exposure are: (a) two weeks of drying in room climate followed by one week's storage in tap water, (b) one week of storage in tap water, (c) one day's membrane hardening.

SRPC with 5% silica	D_{eff}^* (m ² /s)	D_{eff} (m ² /s)	$d_{0.1}$ (mm)
w/b 0.35 (a)	$1.93 \cdot 10^{-12}$	$1.24 \cdot 10^{-12}$	6.3
w/b 0.40 (a)	$3.19 \cdot 10^{-12}$	$1.73 \cdot 10^{-12}$	8.0
w/b 0.55 (a)	$6.64 \cdot 10^{-12}$	$3.68 \cdot 10^{-12}$	8.3
w/b 0.35 (b)	$1.78 \cdot 10^{-12}$	$1.90 \cdot 10^{-12}$	9.1
w/b 0.40 (b)	$2.40 \cdot 10^{-12}$	$2.78 \cdot 10^{-12}$	11.0
w/b 0.55 (b)	$2.72 \cdot 10^{-12}$	$3.78 \cdot 10^{-12}$	13.1
w/b 0.35 (c)	$2.12 \cdot 10^{-12}$	$2.30 \cdot 10^{-12}$	9.1
w/b 0.40 (c)	$2.55 \cdot 10^{-12}$	$2.56 \cdot 10^{-12}$	11.6
w/b 0.55 (c)	$3.84 \cdot 10^{-12}$	$3.86 \cdot 10^{-12}$	13.7

the time scale in the problem. Using longer exposure times than those in the experiments, the depth at which the chloride content reaches its maximum is expected to increase. This is a conclusion drawn from simulations performed using the material constants which gave the best fit to the measured data valid after approximately four months of exposure.

It was seen that the behavior of having a maximum in the chloride profile a few millimeters from the exposed surfaces was most dominant for samples dried in room climate for two weeks followed by one week submerged in tap water before being exposed to chlorides. Furthermore, this behavior was observed for the two highest tested water to binder ratios exposed to chlorides after one day of membrane hardening.

No special attention has been paid in the proposed model to changes of material properties caused by hydration during the chloride exposure. Therefore, the obtained values of material constants, such as the tortuosity factor, the binding capacity and the binding rate must be seen as averaged values valid for an exposure time of approximately four months, as used in the experiments. Even during this relatively long test period the averaged material constants became significantly different for different curing conditions when using the same chloride exposure periods. It is, therefore, concluded

that hydration of samples, during the time of exposure to chlorides in the actual experiments, can only give small changes of the chemical and physical structure obtained already before the time of exposure. Furthermore, it is concluded that the degree of hydration at the time of exposure to chlorides correlates badly with the penetration ability of chlorides, especially when considering samples dried before exposure. The pattern found was that a period of drying before exposure of chlorides heavily reduces the penetration of chlorides, and the actual degree of hydration at the time of exposure was shown to be of less importance compared to the drying effect. A model where the effective diffusion coefficient is allowed to be a function of the current hydration degree only is, therefore, concluded to be too simplified. It seems that the micro-structural effects in the concrete caused by drying at early ages must be included in the model as a major factor influencing chloride penetration.

The model suggested to describe chloride penetration into concrete accounts for effects of the concentration of different types of ions in the pore solution and in the storage solution on the chloride ingress. It can not, therefore, be directly concluded that samples which were less penetrated by chlorides, i.e., in this case, samples dried and rewetted with tap water before exposure to a sodium chloride solution, have the most dense micro-structure. The reason for a higher chloride penetration resistance might also be that the composition of pore solution becomes different when the sample has been subjected to drying before exposure.

A stringent verification of the proposed model requires the experimental observations of concentration fields of all different types of ions present in the pore solution under different exposure conditions. In this study only the chloride ion concentration profiles were measured. A natural extension is, therefore, to measure profiles for ions other than chlorides. The results from such measurements should be compared with the results given by the model. Another interesting study is to measure profiles at different times from exposure. This makes it possible to check how well the model simulates the development of concentration fields with time. Naturally, this is a very important issue.

References

- [1] Glass, G.K., Hassanein, N.M. and Buenfeld, N.R. (1997). *Neural Net-*

- work Modelling of Chloride Binding*. Magazine of Concrete Research, V. 49, No. 181, pp. 323-335.
- [2] Mangat, P.S. and Molloy, B.T. (1995). *Chloride Binding in Concrete Containing PFA, gbs or Silica Fume under Sea Water Exposure*, Cement and Concrete Research, Vol. 47, No. 171, pp. 129-141.
- [3] Wee, T.H., Wong, S.F., Swaddiwudhipong, S. and Lee, S.L. (1997). *A Prediction Method for Long-Term Chloride Concentration Profiles in Hardening Cement Matrix Materials*. ACI Materials Journal, Vol. 94, No. 6, pp. 565-579.
- [4] Dhir, R.K., Hewlett, P.C. and Dyer, T.D. (1999). *Chemical Profiles of Cement Pastes Exposed to a Chloride Solution Spray*, Cement and Concrete Research, Vol. 29, pp. 667-672.
- [5] Bowen, R.M. (1976). *Theory of Mixtures*, Part 1, in Continuum Physics, Edited by A. Cemal Erigen, Princeton University of Technology.
- [6] Weast, R.C., Lide, D.R. Astle, M.J. and Beyer, W.H. (1989). *Handbook of Chemistry and Physics*, 70TH edition, CRC Press, Inc. Boca Raton, Florida.
- [7] Atkins, P.W. (1994). *Physical Chemistry*, Fifth Edition, Oxford University Press; Oxford.
- [8] Zienkiewicz, O.C. and Taylor, R.L. (1989). *The Finite Element Method, Fourth Edition*, Vol. 2, McGraw-Hill, London.
- [9] Bathe, K.J. (1996). *The Finite Element Procedures*, Prentice Hall, Englewood Cliffs, New Jersey.
- [10] Hughes, T.J.R. (1987). *The Finite Element Method, Linear Static and Dynamic Finite Element Analysis*, Prentice-Hall International Editions.
- [11] Sharif, A. A., Loughlin K.F. Azad, A.K. and Navaz, C.M. (1997). *Determination of the Effective Chloride Diffusion Coefficient in Concrete via a Gas Diffusion Technique*, ACI Materials Journal, Vol. 94, No. 3, pp. 227-233.

- [12] Samson, E., Marchand, J. and Beaudoin, J.J. (1999). *Describing Ion Diffusion Mechanisms in Cement-Based Materials using the Homogenization Technique*. Cement and Concrete Research, Vol. 29, pp. 1341-1345.